

A Family of Horizon-penetrating Characteristic Coordinate Systems for the Schwarzschild Geometry

Christian Röken^{1,2}

¹*Departamento de Geometría y Topología, Facultad de Ciencias - Universidad de Granada, Campus de Fuentenueva s/n, 18071 Granada, Spain*

²*Rheinische Friedrichs-Wilhelms-Universität Bonn, Philosophische Fakultät, Institut für Philosophie, 53113 Bonn, Germany*

(Dated: September 2020)

ABSTRACT. We introduce a new family of horizon-penetrating coordinate systems for the analytic extension of the Schwarzschild geometry across the event horizon that feature time coordinates, which are Cauchy temporal functions, i.e., the level sets of these time coordinates are smooth, spacelike Cauchy hypersurfaces. Such coordinate systems are well suited for the initial value formulation and for the study of causal and conformally invariant elements associated to the extended Schwarzschild geometry in terms of data on a Cauchy surface. For the construction, we use a basic, fully geometric method that employs structures inherent in the Carter–Penrose diagram of the extended Schwarzschild geometry. This method can be adapted to yield similar coordinate systems for various other geometries as well.

Contents

I. Introduction	2
II. Preliminaries	3
A. Maximal Analytic Extension of the Schwarzschild Geometry: Compactified Kruskal–Szekeres Coordinates	3
B. Carter–Penrose Diagram of the Schwarzschild Geometry	5
C. Cauchy Surfaces and Time-type Functions	7
III. Construction of a Family of Horizon-penetrating Characteristic Coordinate Systems for the Schwarzschild Geometry	7
IV. Application to Sigmoid Functions	11
V. The Minkowski Limit	13
VI. Generalization to the Nonextreme Reissner–Nordström Geometry	14
VII. Summary and Outlook	17
Acknowledgments	17
References	17

I. INTRODUCTION

In a certain class of 4-dimensional Lorentzian manifolds, there exist preferred 2-dimensional submanifolds with induced metrics that are locally and conformally equivalent to the actual Lorentzian metrics. These submanifolds may be used to analyze the global causal structures of the underlying Lorentzian manifolds. For first applications of this approach to the Schwarzschild, Reissner–Nordström, and Kerr geometries, we refer the reader to, e.g., [5, 6, 14, 17, 21]. As can be seen, i.a., from these first applications, one of the most prominent examples of these preferred 2-dimensional submanifolds are the 2-surfaces containing the two double principal null directions in a Petrov type D solution of the vacuum Einstein field equations in general relativity [18, 34], which can be employed to study the causal structures of black hole geometries, for instance by means of Carter–Penrose diagrams [11, 32]. Furthermore, this concept of analyzing the causal structures of Lorentzian manifolds is particularly useful in the context of global hyperbolicity, which is a specific condition on the causal structures of Lorentzian manifolds that gives rise to foliations by smooth, spacelike Cauchy hypersurfaces. Thus, it is relevant for the initial value formulation of the Einstein field equations, where one derives solutions by prescribing initial data on a given spacelike Cauchy hypersurface and evolves this data along the other Cauchy hypersurfaces forward and backward in time. In this regard, it was shown in [9] that the set of maximal globally hyperbolic extensions of the above Petrov type D solutions are uniquely determined, up to isometry, by initial data specified on some spacelike Cauchy hypersurface. It is hence instructive to study the causal structures and certain aspects of the initial value formulations of such extensions via the 2-dimensional approach.

In this work, we focus on a 2-dimensional construction procedure for coordinate systems that are suitable for the initial value formulations of specific analytic extensions of the family of spherically symmetric Petrov type D solutions of the vacuum Einstein field equations, which are, according to Birkhoff’s theorem, isometric to a subset of the maximally extended Schwarzschild solution. This solution may be used in order to describe the final equilibrium state of the dynamical evolution of the exterior gravitational field of an isolated, spherically symmetric body like, e.g., a compact star or a nonrotating, uncharged black hole (we here focus on the latter). To be more precise, the Schwarzschild solution constitutes a 1-parameter family of spherically symmetric solutions of the vacuum Einstein field equations $\text{Ric}(\mathbf{g}) = \mathbf{0}$, where spherical symmetry is defined as follows.

Definition I.1. *We let $(\mathfrak{M}, \mathbf{g})$ be a 4-dimensional Lorentzian manifold. Then, $(\mathfrak{M}, \mathbf{g})$ is called spherically symmetric if the special orthogonal group $\text{SO}(3)$ acts as a group of isometries $\mathfrak{I}: \mathfrak{M} \times \text{SO}(3) \rightarrow \mathfrak{M}$ with spacelike, codimension-2 orbits homeomorphic to S^2 .*

The quotient $\mathfrak{M}/\text{SO}(3)$ is a 2-dimensional manifold without boundary, homeomorphic to \mathbb{R}^2 . Moreover, the Schwarzschild solution and its maximal analytic extension are globally hyperbolic with a complete, smooth, spacelike Cauchy hypersurface \mathfrak{N} homeomorphic to $\mathbb{R} \times S^2$ [8, 12]. Since every spherically symmetric solution \mathbf{g} of the vacuum Einstein field equations is static, i.e., the associated Lorentzian manifold admits a global, nonvanishing, timelike and irrotational Killing vector field $\mathbf{K} \in \Gamma(T\mathfrak{M})$, it can be written in the local form

$$\mathbf{g} = \alpha(\mathbf{x}) dt \otimes dt - \mathbf{g}_{\mathfrak{N}},$$

where $(t, \mathbf{x}) \in \mathbb{R} \times \mathfrak{N} \cong \mathfrak{M}$, $\alpha: \mathfrak{N} \rightarrow \mathbb{R}_{>0}$, and $\mathbf{g}_{\mathfrak{N}}$ is the induced Riemannian metric on \mathfrak{N} . Given that $\mathfrak{N} \cong \mathbb{R} \times S^2$, we can in addition express the induced Riemannian metric as $\mathbf{g}_{\mathfrak{N}} = \beta(\mathbf{x}) dr \otimes dr + \gamma(\mathbf{x}) \mathbf{g}_{S^2}$, with $r \in \mathbb{R}_{>0}$ being a radial coordinate, $\beta, \gamma: \mathfrak{N} \rightarrow \mathbb{R}_{>0}$, and \mathbf{g}_{S^2} denoting the metric on S^2 . This particular product structure allows us to consider the quotient $\mathfrak{M}/\text{SO}(3)$, and therefore 2-dimensional Carter–Penrose diagrams, as the basis for a geometric construction procedure for a family of regular coordinate systems that cover the analytic extension of the Schwarzschild geometry across the event horizon and feature time coordinates that are temporal functions for which the level sets

are smooth, asymptotically flat, spacelike Cauchy hypersurfaces. For the construction and study of alternative coordinate systems for the Schwarzschild geometry that rely on 2-dimensional conformal compactifications see, e.g., [1, 20] for coordinates that yield complete spacelike hypersurfaces, which simultaneously extend smoothly through the event horizon and intersect null infinity.

The paper is organized as follows. In Section II, we recall some basics of the Schwarzschild geometry and its maximal analytic extension, the construction of the Carter–Penrose diagram of the analytic extension of the Schwarzschild geometry across the event horizon, as well as Cauchy surfaces and time-type functions in general. Subsequently, in Section III, we present a geometric method of construction for obtaining a family of horizon-penetrating characteristic coordinate systems for the Schwarzschild geometry (for a motivation of the terminology *characteristic* see the end of Section II C), which employs the geometry of Carter–Penrose diagrams, affine as well as homotopy transformations, and foliations by indexed families of smooth functions. We also prove that the level sets of the time variables of these coordinate systems are smooth, spacelike Cauchy hypersurfaces. An application using sigmoid functions is given in Section IV. In Sections V and VI, we analyze the possibility of performing the Minkowski limit and generalize our results to the analytic extension of the nonextreme Reissner–Nordström geometry up to the Cauchy horizon, respectively. Finally, we conclude with a summary of our results and a brief discussion of future research projects in Section VII.

II. PRELIMINARIES

We summarize the main geometrical and topological aspects of the Schwarzschild geometry and present a derivation of compactified Kruskal–Szekeres coordinates, which cover the maximal analytic extension of this geometry. We then give an account of the construction of the Carter–Penrose diagram of the analytic extension of the Schwarzschild geometry across the event horizon. Finally, we briefly recall the notions of Cauchy surfaces and time-type functions.

A. Maximal Analytic Extension of the Schwarzschild Geometry: Compactified Kruskal–Szekeres Coordinates

The Schwarzschild geometry $(\mathfrak{M}, \mathbf{g})$ is a smooth, asymptotically flat and globally hyperbolic Lorentzian 4-manifold, with \mathfrak{M} being homeomorphic to $\mathbb{R}^2 \times S^2$ and a – up to the event horizon – spherically symmetric, static metric \mathbf{g} , which constitutes a 1-parameter family of solutions of the vacuum Einstein field equations. Furthermore, this metric is algebraically special, more precisely, it is of Petrov type D. In the standard Schwarzschild coordinates $(t, r, \theta, \varphi) \in \mathbb{R} \times \mathbb{R}_{>0} \times (0, \pi) \times [0, 2\pi)$, the Schwarzschild metric takes the form [33]

$$\mathbf{g} = \left[1 - \frac{2M}{r}\right] dt \otimes dt - \left[1 - \frac{2M}{r}\right]^{-1} dr \otimes dr - r^2 \mathbf{g}_{S^2}, \quad (1)$$

in which the parameter $M \in \mathbb{R}_{>0}$ coincides with the ADM mass of the black hole geometry and $\mathbf{g}_{S^2} = d\theta \otimes d\theta + \sin^2(\theta) d\varphi \otimes d\varphi$ is the metric on the unit 2-sphere. It is valid for all $r \in \mathbb{R}_{>0} \setminus \{2M\}$ and features two types of singularities, namely a spacelike curvature singularity at $r = 0$ and a coordinate singularity at $r = 2M$, with the latter being the location of the event horizon $\mathfrak{M} \cap \partial J^-(\mathcal{I}^+)$, that is, the boundary of the causal past of future null infinity. The Schwarzschild geometry may thus be separated into two connected components – the Boyer–Lindquist block $B_I := \mathbb{R} \times \mathbb{R}_{>2M} \times S^2$, which is the domain of outer communication, and $B_{II} := \mathbb{R} \times (0, 2M) \times S^2$, which is the future trapped region or black hole region $\mathfrak{M} \setminus J^-(\mathcal{I}^+) \neq \emptyset$, – at the event horizon [26]. We remark that in the Boyer–Lindquist block B_I , the Schwarzschild time coordinate t is a Cauchy temporal function, i.e., it yields a foliation of this region by smooth, spacelike Cauchy hypersurfaces (see Section II C). However, due to the degeneracy

of the Schwarzschild coordinates at $-$ and the violation of staticity across $-$ the event horizon, the level sets of t do not foliate the analytically extended Schwarzschild geometry $B_I \cup B_{II}$.

We next recall the usual derivation of compactified Kruskal–Szekeres coordinates, which are coordinates that cover the maximal analytic extension of the Schwarzschild geometry. These coordinates give rise to a global foliation by spacelike Cauchy hypersurfaces. They are regular for all values of $r \in \mathbb{R}_{>0}$, locate the event horizon at finite coordinate values, and yield a compactification of the spacetime into a finite domain. Thus, they are suitable coordinates for the construction of the Carter–Penrose diagram of the maximal analytic extension of the Schwarzschild geometry. However, for the purposes of the present work, we restrict them to the region $B_I \cup B_{II}$. Firstly, we remove the Schwarzschild coordinate singularity at the event horizon at $r = 2M$, which manifests itself in the divergence of the g_{rr} component of the metric (1), and hence in the degeneracy of the light cone approaching the event horizon, that is, in the divergence of the quantity $\lim_{r \rightarrow 2M} dt/dr = \pm \lim_{r \rightarrow 2M} \sqrt{-g_{rr}/g_{tt}} = \pm \infty$ along radial null geodesics. To this end, we transform the Schwarzschild coordinates into Eddington–Finkelstein double-null coordinates [13, 14]

$$\mathfrak{T}^{\text{EF}} : \begin{cases} \mathbb{R} \times \mathbb{R}_{>0} \times (0, \pi) \times [0, 2\pi) \rightarrow \mathbb{R} \times \mathbb{R} \times (0, \pi) \times [0, 2\pi) \\ (t, r, \theta, \varphi) \mapsto (u, v, \theta, \varphi) \end{cases}$$

with

$$\begin{cases} u = t - r_\star & \text{and} & v = t + r_\star & \text{for } B_I \\ u = t + r_\star & \text{and} & v = -t + r_\star & \text{for } B_{II}, \end{cases} \quad (2)$$

where

$$r_\star := r + 2M \ln \left| \frac{r}{2M} - 1 \right| \in \begin{cases} \mathbb{R} & \text{for } B_I \\ \mathbb{R}_{<0} & \text{for } B_{II} \end{cases} \quad (3)$$

is the Regge–Wheeler coordinate, and $v - u \in \mathbb{R}$ in B_I as well as $v + u \in \mathbb{R}_{<0}$ in B_{II} . The Schwarzschild metric in Eddington–Finkelstein double-null coordinates reads

$$\mathbf{g} = \frac{1}{2} \left| 1 - \frac{2M}{r} \right| (du \otimes dv + dv \otimes du) - r^2 \mathbf{g}_{S^2}.$$

As these coordinates become constant along the ingoing and outgoing radial null geodesics of the Schwarzschild geometry, the light cone structure at the event horizon now remains regular. However, Eddington–Finkelstein double-null coordinates have the disadvantage that the event horizon is shifted to infinity. Accordingly, we further apply a transformation into the Kruskal–Szekeres double-null coordinate system

$$\mathfrak{T}^{\text{KS1}} : \begin{cases} \mathbb{R} \times \mathbb{R} \times (0, \pi) \times [0, 2\pi) \rightarrow \left(-\frac{\pi}{2}, \frac{\pi}{2}\right) \times \left(0, \frac{\pi}{2}\right) \times (0, \pi) \times [0, 2\pi) \\ (u, v, \theta, \varphi) \mapsto (U, V, \theta, \varphi) \end{cases}$$

with

$$\begin{cases} \tan(U) = -e^{-u/(4M)} & \text{and} & \tan(V) = e^{v/(4M)} & \text{for } B_I \\ \tan(U) = e^{u/(4M)} & \text{and} & \tan(V) = e^{v/(4M)} & \text{for } B_{II}, \end{cases} \quad (4)$$

where $\tan(U) \tan(V) \in \mathbb{R}_{<0}$ in B_I and $\tan(U) \tan(V) \in (0, 1)$ in B_{II} , in which the event horizon is located at finite coordinate values. In addition, these coordinates give rise to a compactification of the

spacetime required for the construction of Carter–Penrose diagrams. Finally, we transform the double-null coordinates (4) into a compactified form of the usual Kruskal–Szekeres spacetime coordinates [21, 35]

$$\mathfrak{T}^{\text{KS2}} : \begin{cases} \left(-\frac{\pi}{2}, \frac{\pi}{2}\right) \times \left(0, \frac{\pi}{2}\right) \times (0, \pi) \times [0, 2\pi) \rightarrow \left(-\frac{\pi}{4}, \frac{\pi}{4}\right) \times \left(-\frac{\pi}{4}, \frac{\pi}{2}\right) \times (0, \pi) \times [0, 2\pi) \\ (U, V, \theta, \varphi) \mapsto (T, X, \theta, \varphi) \end{cases}$$

with

$$T = \frac{U+V}{2} \quad \text{and} \quad X = \frac{-U+V}{2} \quad \text{for } B_{\text{I}} \cup B_{\text{II}}, \quad (5)$$

where $T \in (|X - \pi/4| - \pi/4, -|X - \pi/4| + \pi/4)$ and $X \in (0, \pi/2)$ in B_{I} and $T \in (|X|, \pi/4)$ and $X \in (-\pi/4, \pi/4)$ in B_{II} (cf. TABLE I). Using these coordinates, the Schwarzschild metric can be represented as

$$\mathbf{g} = \frac{32M^3 e^{-r/(2M)}}{\cos^2(U) \cos^2(V) r} (dT \otimes dT - dX \otimes dX) - r^2 \mathbf{g}_{S^2}. \quad (6)$$

Considering the inverse of this metric, it follows from the positivity of the g^{TT} component that $\mathbf{g}(\nabla T, \nabla T) > 0$, and since $\mathbf{g}(\partial_T, \nabla T) > 0$ with ∂_T being timelike in $B_{\text{I}} \cup B_{\text{II}}$, ∇T is future-directed and timelike. Hence, the Kruskal–Szekeres time coordinate T is a temporal function on the analytic extension $B_{\text{I}} \cup B_{\text{II}}$ (see again Section II C). The induced metric on the level sets of T is therefore Riemannian. We point out in passing that instead of employing the above Kruskal–Szekeres coordinates, one may as well work with different types of compactified horizon-penetrating coordinate systems derived from, e.g., Gullstrand–Painlevé coordinates, Lemaître coordinates, or advanced Eddington–Finkelstein coordinates [19, 22, 28]. Furthermore, as the Kruskal–Szekeres coordinates cover the entire maximal analytic extension, they are more general than required. However, they are – and yield representations of geometric quantities that are – nevertheless still fairly simple and easy to handle.

B. Carter–Penrose Diagram of the Schwarzschild Geometry

Due to the particular product structure of the Schwarzschild metric in compactified Kruskal–Szekeres coordinates (6), that is

$$\mathbf{g} = \mathbf{g}_{\text{L}}^{(2)} \oplus \mathbf{g}_{\text{R}}^{(2)} \quad \text{on} \quad \mathfrak{M} = \mathfrak{M}_{\text{L}}^{(2)} \times \mathfrak{M}_{\text{R}}^{(2)} \quad (7)$$

with

$$\mathbf{g}(\mathbf{V}_{\text{L}} + \mathbf{V}_{\text{R}}, \mathbf{W}_{\text{L}} + \mathbf{W}_{\text{R}}) = \mathbf{g}_{\text{L}}^{(2)}(\mathbf{V}_{\text{L}}, \mathbf{W}_{\text{L}}) + \mathbf{g}_{\text{R}}^{(2)}(\mathbf{V}_{\text{R}}, \mathbf{W}_{\text{R}})$$

for

$$\mathbf{V}_{\text{L/R}}, \mathbf{W}_{\text{L/R}} \in \Gamma(T\mathfrak{M}_{\text{L}}^{(2)})/\Gamma(T\mathfrak{M}_{\text{R}}^{(2)}) \quad \text{and the identification} \quad T(\mathfrak{M}_{\text{L}}^{(2)} \times \mathfrak{M}_{\text{R}}^{(2)}) = T\mathfrak{M}_{\text{L}}^{(2)} \oplus T\mathfrak{M}_{\text{R}}^{(2)},$$

where

$$\mathbf{g}_{\text{L}}^{(2)} = \frac{32M^3 e^{-r/(2M)}}{\cos^2(U) \cos^2(V) r} (dT \otimes dT - dX \otimes dX) \quad \text{and} \quad \mathbf{g}_{\text{R}}^{(2)} \cong \mathbf{g}_{S^2}$$

are 2-dimensional Lorentzian and Riemannian metrics on $\mathfrak{M}_{\text{L}}^{(2)} \cong \mathbb{R}^2$ and $\mathfrak{M}_{\text{R}}^{(2)} \cong S^2$, respectively, any causal vector with respect to \mathbf{g} is also a causal vector with respect to $\mathbf{g}_{\text{L}}^{(2)}$ [10, 38]. This makes it

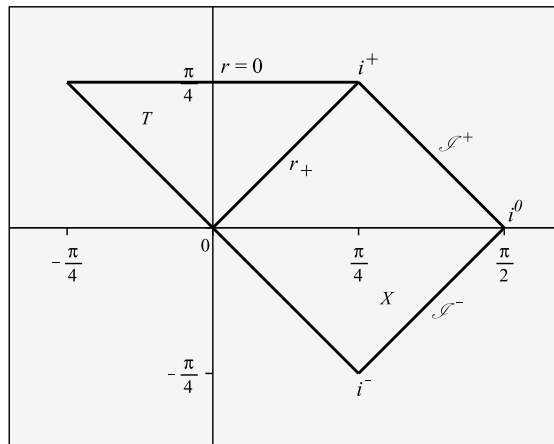


FIG. 1: Carter–Penrose diagram of the analytic extension of the Schwarzschild geometry across the event horizon.

possible to analyze the causal relations between different points in – and thus understanding the global causal structure of – the analytic extension $B_I \cup B_{II}$ of the spherically symmetric Schwarzschild geometry using a 2-dimensional Carter–Penrose diagram, where the metric $g_L^{(2)}$ on this diagram is locally and conformally equivalent to the actual metric g with every point corresponding to a 2-sphere. We note that this equivalency is lost in the case of the more general nonextreme Kerr geometry, as the associated metric does not have the required product structure [26].

For the construction of the Carter–Penrose diagram of the two Boyer–Lindquist blocks $B_I \cup B_{II}$, we employ the relations

$$\left\{ \begin{array}{l} \frac{\sin(2T)}{\sin(2X)} = \tanh(t/(4M)) \quad \text{and} \quad \frac{\cos(2T)}{\cos(2X)} = -\coth(r_*/(4M)) \quad \text{for } B_I \\ \frac{\sin(2T)}{\sin(2X)} = -\coth(t/(4M)) \quad \text{and} \quad \frac{\cos(2T)}{\cos(2X)} = -\tanh(r_*/(4M)) \quad \text{for } B_{II} \end{array} \right.$$

between the Boyer–Lindquist and the Kruskal–Szekeres coordinates, which give rise to the asymptotics shown in TABLE I. These asymptotics may be used to define the relevant structures of the Carter–Penrose diagram, namely future/past timelike infinity $i^\pm = (T = \pm\pi/4, X = \pi/4)$, future/past null infinity $\mathcal{S}^\pm = \{(T, X) | T = \pm(-X + \pi/2) \text{ and } \pi/4 < X < \pi/2\}$, spacelike infinity $i^0 = (T = 0, X = \pi/2)$, the event horizon at $\{(T, X) | T = X \text{ and } 0 \leq X \leq \pi/4\}$, and the location of the curvature singularity at $\{(T, X) | T = \pi/4 \text{ and } -\pi/4 \leq X \leq \pi/4\}$. We depict the Carter–Penrose diagram of the analytic extension $B_I \cup B_{II}$ of the Schwarzschild geometry in FIG. 1.

TABLE I: Relations between Boyer–Lindquist and Kruskal–Szekeres asymptotics.

	$r \rightarrow \infty$	$r \rightarrow 2M$	$r \rightarrow 0$	$t \rightarrow \pm\infty$
B_I	$T = \pm[X - \pi/2]$	$T = \pm X$		$T = \mp[X - \pi/2], T = \pm X$
B_{II}		$T = \pm X$	$T = \pi/4$	$T = \mp X$

C. Cauchy Surfaces and Time-type Functions

For the present purpose of deriving a family of horizon-penetrating characteristic coordinate systems for the Schwarzschild geometry, where the time coordinates are Cauchy temporal functions, we first define the concepts of Cauchy surfaces and time-type functions, beginning with the former.

Definition II.1. *A Cauchy surface of a time-oriented, connected Lorentzian manifold $(\mathfrak{M}, \mathbf{g})$ is any subset $\mathfrak{N} \subset \mathfrak{M}$ that is closed and achronal, and has the domain of dependence $D(\mathfrak{N}) = \mathfrak{M}$, i.e., it is intersected by every inextendible timelike curve exactly once.*

A Cauchy surface is therefore a topological hypersurface [27], which can be approximated by a smooth, spacelike hypersurface [2]. Moreover, in case $(\mathfrak{M}, \mathbf{g})$ admits a Cauchy surface, it is globally hyperbolic [16]. Next, we introduce time-type functions.

Definition II.2. *We let $(\mathfrak{M}, \mathbf{g})$ be a time-oriented, connected Lorentzian manifold. A function $\mathfrak{t}: \mathfrak{M} \rightarrow \mathbb{R}$ is called a*

1. *generalized time function if it is strictly increasing on any future-directed causal curve.*
2. *time function if it is a continuous generalized time function.*
3. *temporal function if it is a smooth function with future-directed, timelike gradient $\nabla \mathfrak{t}$.*

According to [3, 15], there is the following relation between time-type functions and the notion of global hyperbolicity.

Proposition II.3. *Any globally hyperbolic Lorentzian manifold $(\mathfrak{M}, \mathbf{g})$ contains a Cauchy temporal function \mathfrak{t} , that is, a temporal function for which the level sets $\mathfrak{t}^{-1}(\cdot)$ are smooth, spacelike Cauchy hypersurfaces $(\mathfrak{N}_t)_{t \in \mathbb{R}}$ with $\mathfrak{N}_t := \{\mathfrak{t}\} \times \mathfrak{N}$ and $\mathfrak{N}_t \subset J^-(\mathfrak{N}_{t'})$ for all $t < t'$, where $J^-(\cdot)$ denotes the causal past.*

In order to verify whether a given time coordinate \mathfrak{t} is a Cauchy temporal function, we evaluate its gradient

$$\nabla \mathfrak{t} = g^{\mu\nu} (\partial_\mu \mathfrak{t}) \partial_\nu = g^{t\nu} \partial_\nu$$

and subsequently

$$g(\mathbf{Y}, \nabla \mathfrak{t}) = Y^t > 0 \quad \text{as well as} \quad g(\nabla \mathfrak{t}, \nabla \mathfrak{t}) = g^{tt},$$

with $\mathbf{Y} \in \Gamma(T\mathfrak{M})$ being timelike. In case the latter expression turns out to be positive too, we have demonstrated that $\nabla \mathfrak{t}$ is future-directed and timelike, and hence if \mathfrak{t} is smooth, that it is a temporal function. Consequently, the level sets of \mathfrak{t} are spacelike, which can be established by showing that the induced metric on constant- \mathfrak{t} hypersurfaces is Riemannian. Then, we prove that these level sets satisfy the Cauchy property by verifying that they are closed and achronal, and that their total Cauchy horizons are empty. We remark that a coordinate system $(\mathfrak{t}, \mathbf{x})$ on \mathfrak{M} , where $\mathfrak{t} \in \mathbb{R}$ is a Cauchy temporal function and \mathbf{x} are coordinates on $\mathfrak{N}_t \subset \mathfrak{M}$, may be understood as corresponding to an observer who is co-moving along the flow lines of the Killing field $\Gamma(T\mathfrak{M}) \ni \mathbf{K} = \partial_t$, which gives rise to the term *characteristic*.

III. CONSTRUCTION OF A FAMILY OF HORIZON-PENETRATING CHARACTERISTIC COORDINATE SYSTEMS FOR THE SCHWARZSCHILD GEOMETRY

We derive a family of characteristic coordinate systems for the analytic extension of the Schwarzschild geometry across the event horizon $B_I \cup B_{II}$, which are regular in the entire domain and feature time

coordinates that are Cauchy temporal functions, i.e., these coordinate systems yield foliations of the extended Schwarzschild geometry by smooth, spacelike Cauchy hypersurfaces. For this purpose, we make use of the particular product structure (7) of the Schwarzschild metric, which allows us to employ a method of construction that relies only on geometric structures inherent in the Carter–Penrose diagram of the extended Schwarzschild geometry as follows.

Firstly, to simplify the geometrical shape of the Carter–Penrose diagram, we transform the Schwarzschild trapezoid shown in FIG. 2(a) into a centrally symmetric diamond as in FIG. 2(f). To this end, we align the line connecting i^0 and the point $(T = \pi/4, X = -\pi/4)$ with the abscissa using rotation and translation transformations, apply a homotopy transformation in order to deform the trapezoid into a rectangle, and attain central symmetry – and hence a diamond – via a shear mapping (see the steps in FIG. 2). Secondly, we present a procedure for the construction of indexed families of smooth functions that all start at i^0 and end at $(T = \pi/4, X = -\pi/4)$, correspond to asymptotically flat, spacelike Cauchy hypersurfaces in $B_I \cup B_{II}$, and fill the entire diamond. Finally, we use these indexed families for the definition of regular coordinate systems suitable for foliating the extended Schwarzschild geometry, where the indices serve as new time variables. In more detail, we first rotate the Schwarzschild trapezoid counter-clockwise about an angle of 45° (FIG. 2(a) \rightarrow FIG. 2(b)) employing the transformation

$$\mathfrak{T}^{(1)} : \begin{cases} \left(-\frac{\pi}{4}, \frac{\pi}{4}\right) \times \left(-\frac{\pi}{4}, \frac{\pi}{2}\right) \rightarrow \left(0, \frac{\pi}{2\sqrt{2}}\right) \times \left(-\frac{\pi}{2\sqrt{2}}, \frac{\pi}{2\sqrt{2}}\right) \\ (T = T^{(0)}, X = X^{(0)}) \mapsto (T^{(1)}, X^{(1)}) \end{cases} \quad (8)$$

with

$$T^{(1)} = \frac{T^{(0)} + X^{(0)}}{\sqrt{2}} \quad \text{and} \quad X^{(1)} = \frac{-T^{(0)} + X^{(0)}}{\sqrt{2}},$$

where $T^{(1)} < X^{(1)} + \pi/(2\sqrt{2})$ for $-\pi/(2\sqrt{2}) < X^{(1)} \leq 0$. We then deform the resulting trapezoid into a rectangle (FIG. 2(b) \rightarrow FIG. 2(c)) by identifying the line $\{(T^{(1)}, X^{(1)}) \mid T^{(1)} = X^{(1)} + \pi/(2\sqrt{2}) \text{ and } -\pi/(2\sqrt{2}) \leq X^{(1)} \leq 0\}$ with the line $\{(T^{(1)}, X^{(1)}) \mid 0 \leq T^{(1)} \leq \pi/(2\sqrt{2}) \text{ and } X^{(1)} = -\pi/(2\sqrt{2})\}$ by applying the transformation

$$\mathfrak{T}^{(2)} : \begin{cases} \left(0, \frac{\pi}{2\sqrt{2}}\right) \times \left(-\frac{\pi}{2\sqrt{2}}, \frac{\pi}{2\sqrt{2}}\right) \rightarrow \left(0, \frac{\pi}{2\sqrt{2}}\right) \times \left(-\frac{\pi}{2\sqrt{2}}, \frac{\pi}{2\sqrt{2}}\right) \\ (T^{(1)}, X^{(1)}) \mapsto (T^{(2)}, X^{(2)}) \end{cases} \quad (9)$$

with

$$T^{(2)} = T^{(1)} \quad \text{and} \quad X^{(2)} = \frac{T^{(1)}/2 - X^{(1)}}{T^{(1)}\sqrt{2}/\pi - 1}.$$

Next, we use a translation by $-\pi/(4\sqrt{2})$ along the ordinate (FIG. 2(c) \rightarrow FIG. 2(d)) and a clockwise rotation about an angle of $\arctan(1/2)$ (FIG. 2(d) \rightarrow FIG. 2(e)), implemented by means of the mappings

$$\mathfrak{T}^{(3)} : \begin{cases} \left(0, \frac{\pi}{2\sqrt{2}}\right) \times \left(-\frac{\pi}{2\sqrt{2}}, \frac{\pi}{2\sqrt{2}}\right) \rightarrow \left(-\frac{\pi}{4\sqrt{2}}, \frac{\pi}{4\sqrt{2}}\right) \times \left(-\frac{\pi}{2\sqrt{2}}, \frac{\pi}{2\sqrt{2}}\right) \\ (T^{(2)}, X^{(2)}) \mapsto (T^{(3)}, X^{(3)}) \end{cases} \quad (10)$$

with

$$T^{(3)} = T^{(2)} - \frac{\pi}{4\sqrt{2}} \quad \text{and} \quad X^{(3)} = X^{(2)}$$

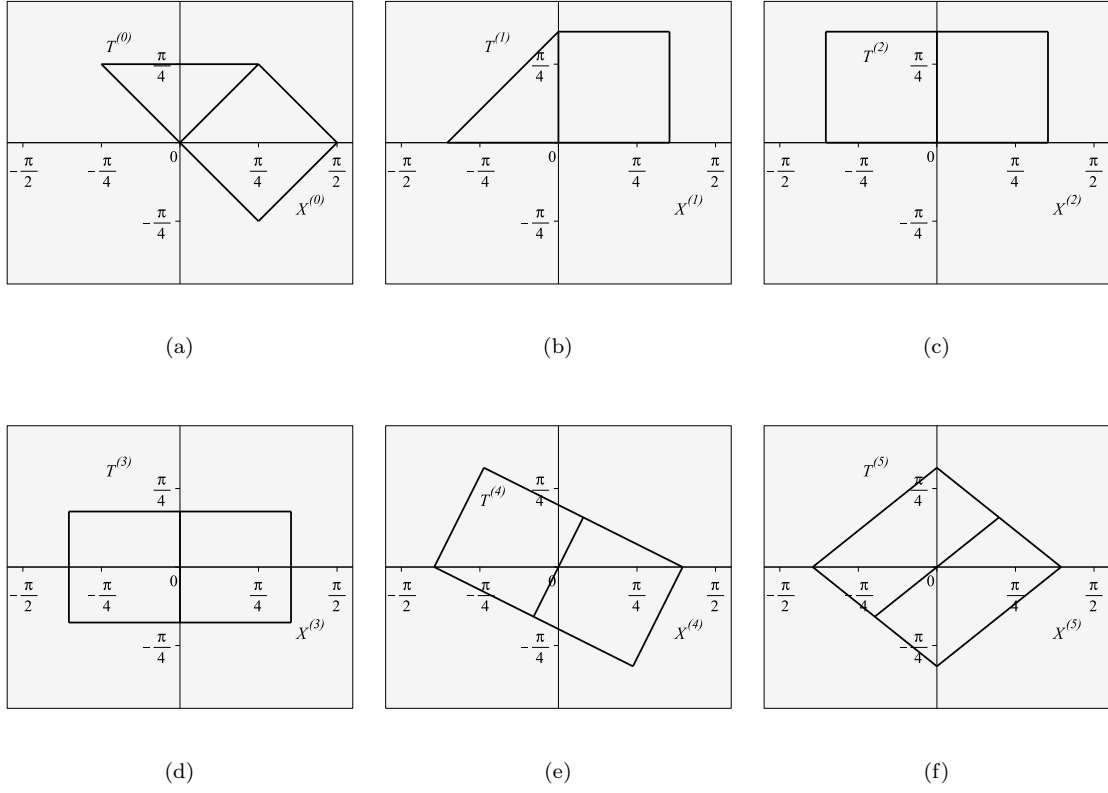


FIG. 2: Exact geometrical representation of the composition of the transformations (8)-(12).

as well as

$$\mathfrak{T}^{(4)} : \begin{cases} \left(-\frac{\pi}{4\sqrt{2}}, \frac{\pi}{4\sqrt{2}} \right) \times \left(-\frac{\pi}{2\sqrt{2}}, \frac{\pi}{2\sqrt{2}} \right) \rightarrow \left(-\frac{\pi}{\sqrt{10}}, \frac{\pi}{\sqrt{10}} \right) \times \left(-\sqrt{\frac{5}{2}} \frac{\pi}{4}, \sqrt{\frac{5}{2}} \frac{\pi}{4} \right) \\ (T^{(3)}, X^{(3)}) \mapsto (T^{(4)}, X^{(4)}) \end{cases} \quad (11)$$

with

$$T^{(4)} = \frac{2T^{(3)} - X^{(3)}}{\sqrt{5}} \quad \text{and} \quad X^{(4)} = \frac{T^{(3)} + 2X^{(3)}}{\sqrt{5}},$$

where

$$\begin{aligned} T^{(4)} < H\left(X^{(4)} + \sqrt{\frac{5}{2}} \frac{\pi}{4}\right) H\left(-\frac{3\pi}{4\sqrt{10}} - X^{(4)}\right) \left[2X^{(4)} + \sqrt{\frac{5}{2}} \frac{\pi}{2}\right] \\ + H\left(X^{(4)} + \frac{3\pi}{4\sqrt{10}}\right) H\left(\sqrt{\frac{5}{2}} \frac{\pi}{4} - X^{(4)}\right) \frac{1}{2} \left[-X^{(4)} + \sqrt{\frac{5}{2}} \frac{\pi}{4}\right] \end{aligned}$$

and

$$\begin{aligned} - H\left(X^{(4)} + \sqrt{\frac{5}{2}} \frac{\pi}{4}\right) H\left(\frac{3\pi}{4\sqrt{10}} - X^{(4)}\right) \frac{1}{2} \left[X^{(4)} + \sqrt{\frac{5}{2}} \frac{\pi}{4}\right] \\ + H\left(X^{(4)} - \frac{3\pi}{4\sqrt{10}}\right) H\left(\sqrt{\frac{5}{2}} \frac{\pi}{4} - X^{(4)}\right) \left[2X^{(4)} - \sqrt{\frac{5}{2}} \frac{\pi}{2}\right] < T^{(4)}, \end{aligned}$$

respectively. Finally, we employ the shear transformation

$$\mathfrak{T}^{(5)} : \begin{cases} \left(-\frac{\pi}{\sqrt{10}}, \frac{\pi}{\sqrt{10}} \right) \times \left(-\sqrt{\frac{5}{2}} \frac{\pi}{4}, \sqrt{\frac{5}{2}} \frac{\pi}{4} \right) \rightarrow \left(-\frac{\pi}{\sqrt{10}}, \frac{\pi}{\sqrt{10}} \right) \times \left(-\sqrt{\frac{5}{2}} \frac{\pi}{4}, \sqrt{\frac{5}{2}} \frac{\pi}{4} \right) \\ (T^{(4)}, X^{(4)}) \mapsto (T^{(5)}, X^{(5)}) \end{cases} \quad (12)$$

with

$$V = T^{(5)} = T^{(4)} \quad \text{and} \quad W = X^{(5)} = \frac{3T^{(4)}}{4} + X^{(4)},$$

where $4|X^{(5)}|/5 - \pi/\sqrt{10} < T^{(5)} < -4|X^{(5)}|/5 + \pi/\sqrt{10}$, in order to obtain the centrally symmetric diamond (FIG. 2(e) \rightarrow FIG. 2(f)). The composition of the transformations (8)-(12) yields the relations

$$V = \frac{2}{\sqrt{10}[\pi - X - T]} \left(-(X + T)^2 + \pi \left[X + 2T - \frac{\pi}{4} \right] \right) \quad (13)$$

$$W = \frac{5}{2\sqrt{10}[\pi - X - T]} \left(-(X + T)^2 + \frac{\pi}{2} \left[3X + T - \frac{\pi}{2} \right] \right), \quad (14)$$

linking the coordinates (T, X) to the coordinates (V, W) . Then, for the derivation of the indexed families of smooth functions $(V_\lambda(W) | \lambda \in \mathbb{R})$ that fill the diamond, we impose the following requirements:

- (C1) Boundary condition: $V_{\pm\infty}(W) = \pm \frac{4}{5}[-|W| + \mu]$
- (C2) Intersection condition: $V_\lambda(\pm\mu) = 0 \quad \forall \lambda \in \mathbb{R}$
- (C3) Smoothness condition: $V_{|\lambda|<\infty}(W) \in C^\infty((-\mu, \mu), \mathbb{R})$
- (C4) Lapse conditions: $\mathbf{g}(\partial_\lambda, \nabla\lambda) > 0$ and $\mathbf{g}(\nabla\lambda, \nabla\lambda) > 0$
- (C5) Symmetry condition: $\lambda \mapsto -\lambda \Leftrightarrow (V_\lambda, W) \mapsto (-V_\lambda, W)$,

where $\mu := \sqrt{5/2}\pi/4$. We point out that the intersection condition (C2) at $W = +\mu$ gives rise to asymptotic flatness. Furthermore, the lapse conditions (C4) constrain the change of the functions along the index λ , i.e, the transition from $V_\lambda(W)$ to $V_{\lambda'}(W)$ for any $\lambda < \lambda'$, to be future-directed and timelike everywhere. This guarantees, on the one hand, that they do not intersect, except for the points $(V_\lambda, W) = (0, \pm\mu)$, and on the other hand, that their causal character is – and remains – spacelike. The latter statement is, however, only true if one considers families of proper (single-valued) functions instead of families of curves in general, making sure that multivaluedness, which may cause, e.g., hairpin-like turns and to that end lead to changes in the causal character, does not occur. Also, the reflection symmetry provided by the symmetry condition (C5) is not strictly required. Next, considering an index λ that is in accordance with (C1)-(C5) as the new time variable, we define the coordinate transformation

$$\mathfrak{T}^{\text{CC}} : \begin{cases} \left(-\frac{\pi}{4}, \frac{\pi}{4} \right) \times \left(-\frac{\pi}{4}, \frac{\pi}{2} \right) \times (0, \pi) \times [0, 2\pi] \rightarrow \mathbb{R} \times \left(-\frac{\pi}{4}, \frac{\pi}{2} \right) \times (0, \pi) \times [0, 2\pi] \\ (T, X, \theta, \varphi) \mapsto (\lambda, X', \theta, \varphi) \end{cases}$$

with

$$\lambda = \lambda(T, X) \quad \text{and} \quad X' = X.$$

We now prove that the level sets of λ , which are by construction smooth, regular at the event horizon, and asymptotically flat, constitute spacelike Cauchy hypersurfaces in $B_I \cup B_{II}$.

Theorem III.1. *Let $\mathfrak{S} \equiv \mathfrak{S}_{\lambda_0}$ be homeomorphic to the subset*

$$\{\lambda_0\} \times \left(-\frac{\pi}{4}, \frac{\pi}{2}\right) \times S^2 \subset B_I \cup B_{II}$$

of the analytic extension of the Schwarzschild geometry across the event horizon, which is a level set of the time coordinate λ at $\lambda_0 = \text{const.}$ Then, \mathfrak{S} is a spacelike Cauchy hypersurface.

Proof. We begin by showing that \mathfrak{S} is spacelike. To this end, we make use of the fact that the second lapse condition $\mathbf{g}(\nabla\lambda, \nabla\lambda) = g^{\lambda\lambda} > 0$ defined in (C4) gives rise to the relation

$$|\partial_T\lambda| > |\partial_X\lambda|. \quad (15)$$

Employing the Cauchy–Schwarz inequality, we thus obtain

$$1 > |\partial_T\lambda|^{-1} |\partial_X\lambda| > |(\partial_T\lambda)^{-1} \partial_X\lambda| = |\partial_{X'}T|,$$

where the last step is derived from $\partial_{X'}\lambda = 0$ together with the chain rule for $\lambda = \lambda(T, X)$. It can be easily verified that this inequality is equivalent to $g_{X'X'} < 0$, and hence the induced metric $i^*\mathbf{g}$ on \mathfrak{S} is Riemannian. Here, $i: \mathfrak{S} \rightarrow B_I \cup B_{II}$ is a smooth embedding map and the asterisk denotes the pullback. This proves that \mathfrak{S} is spacelike. Next, we establish that \mathfrak{S} is a Cauchy surface. Firstly, as the complement

$$\mathfrak{S}^c \cong \mathbb{R} \setminus \{\lambda_0\} \times \left(-\frac{\pi}{4}, \frac{\pi}{2}\right) \times S^2$$

is open in $B_I \cup B_{II}$, we know that \mathfrak{S} is closed. Secondly, since, according to the conditions (C4), the time coordinate λ is a temporal function on $B_I \cup B_{II}$, that is, $B_I \cup B_{II}$ is stably causal [24], any connected causal curve through this region can intersect \mathfrak{S} at most once. Thus, \mathfrak{S} is achronal. Finally, it remains to be shown that the domain of dependence $D(\mathfrak{S}) = B_I \cup B_{II}$. For this purpose, it suffices to demonstrate that the total Cauchy horizon $H(\mathfrak{S})$ of \mathfrak{S} is empty. This may be accomplished using a proof by contradiction as follows. We suppose that there exists a point p in the future Cauchy horizon $H^+(\mathfrak{S})$. Since \mathfrak{S} is achronal and edgeless, p is the future endpoint of a null geodesic $\gamma \subset H^+(\mathfrak{S})$, which is past inextendible in $B_I \cup B_{II}$ [36]. From this it follows that $\gamma \subset J^+(\mathfrak{S}) \cap J^-(p)$. As $B_I \cup B_{II}$ is globally hyperbolic [8], $J^+(\mathfrak{S}) \cap J^-(p)$ is contained in a compact set. And given that γ cannot be imprisoned in a compact set on which stably causality holds [23], we are led to a contradiction. As a consequence, $H^+(\mathfrak{S}) = \emptyset$. Due to time duality, we can assert that the same holds true for $H^-(\mathfrak{S})$, and therefore $H(\mathfrak{S}) = \emptyset$. ■

IV. APPLICATION TO SIGMOID FUNCTIONS

In this section, we determine a few simple examples of the family $(V_\lambda(W) | \lambda \in \mathbb{R})$ using sigmoid functions. To be more precise, as the compactified analytic extension $B_I \cup B_{II}$ of the Schwarzschild geometry is enclosed by a centrally symmetric diamond (cf. FIG. 2(f)), we are interested in smooth approximations of the absolute value function $|W|$ (see condition (C1)). By considering, e.g., the derivative of the absolute value function, namely the signum function $\text{sgn}(W)$, we may find smooth approximations in terms of sigmoid functions such as

$$\text{sgn}(W) = \lim_{\lambda \rightarrow \infty} \begin{cases} \tanh(\lambda W) & \text{(hyperbolic tangent)} \\ \frac{2}{\pi} \arctan(\lambda W) & \text{(arctangent function)} \\ \frac{\lambda W(2 + \lambda^2 W^2)}{(1 + \lambda^2 W^2)^{3/2}} \quad \text{or} \quad \frac{\lambda W}{\sqrt{1 + \lambda^2 W^2}} & \text{(algebraic functions).} \end{cases}$$

Imposing condition (C1) as well as conditions (C2) and (C5), we then obtain

$$V_\lambda(W) = \frac{4}{5\lambda} \ln \left(\frac{\cosh(\lambda\mu)}{\cosh(\lambda W)} \right)$$

$$V_\lambda(W) = \frac{8}{5\pi} \left[\mu \arctan(\lambda\mu) - W \arctan(\lambda W) - \frac{1}{2\lambda} \ln \left(\frac{1 + \lambda^2 \mu^2}{1 + \lambda^2 W^2} \right) \right]$$

$$V_\lambda(W) = \frac{4\lambda}{5} \left[\frac{\mu^2}{\sqrt{1 + \lambda^2 \mu^2}} - \frac{W^2}{\sqrt{1 + \lambda^2 W^2}} \right]$$

and

$$V_\lambda(W) = \frac{4}{5\lambda} \left[\sqrt{1 + \lambda^2 \mu^2} - \sqrt{1 + \lambda^2 W^2} \right], \quad (16)$$

respectively, by means of integration. We point out that these expressions trivially satisfy condition (C3), as they are based on smooth sigmoid function approximations. Furthermore, the conditions (C4) can in general be verified only a posteriori. In the following, we work out the horizon-penetrating characteristic coordinate system and the metric representation associated with the example defined by formula (16) (for an illustration see FIG. 3(a)) in more detail, as this is the only of the above examples that is analytically invertible with respect to λ and thus makes a full analytic treatment possible in the first place. Therefore, inverting (16) with respect to λ gives rise to a transformation from the Kruskal–Szekeres coordinate system into a new horizon-penetrating characteristic coordinate system for the extended Schwarzschild geometry

$$\mathfrak{T}^{\text{CCS}} : \begin{cases} \left(\left(-\frac{\pi}{4}, \frac{\pi}{4} \right) \times \left(-\frac{\pi}{4}, \frac{\pi}{2} \right) \times (0, \pi) \times [0, 2\pi] \rightarrow \mathbb{R} \times \left(-\frac{\pi}{4}, \frac{\pi}{2} \right) \times (0, \pi) \times [0, 2\pi] \right. \\ \left. (T, X, \theta, \varphi) \mapsto (\lambda, X', \theta, \varphi) \right. \end{cases}$$

with

$$\lambda = \frac{5V(T, X)}{2\sqrt{\left[W(T, X)^2 - \frac{25V(T, X)^2}{16} + \frac{5\pi^2}{32} \right]^2 - \frac{5\pi^2 W(T, X)^2}{8}}} \quad \text{and} \quad X' = X, \quad (17)$$

in which the functions $V(T, X)$ and $W(T, X)$ are specified in (13) and (14), respectively. The Schwarzschild metric expressed via these particular characteristic coordinates reads

$$\mathbf{g} = \frac{32M^3 e^{-r/(2M)}}{[15\pi\lambda + \sqrt{160 + 25\pi^2\lambda^2}]^4 \cos^2(U) \cos^2(V) r} \left[400\pi^2 \mathcal{C}_\lambda^2 d\lambda \otimes d\lambda - 40\pi \mathcal{C}_\lambda \mathcal{C}_{X'} \right. \\ \left. \times (d\lambda \otimes dX' + dX' \otimes d\lambda) + (4\mathcal{C}_{X'}^2 - [15\pi\lambda + \sqrt{160 + 25\pi^2\lambda^2}]^4) dX' \otimes dX' \right] - r^2 \mathbf{g}_{S^2},$$

where

$$\mathcal{C}_\lambda := \frac{20[4X' - 5\pi]}{\sqrt{160 + 25\pi^2\lambda^2}} - \frac{\sqrt{5\pi}}{\sqrt{5\pi\lambda^2[X' - \pi/4]^2 - 2[4X' - 3\pi]}} \left(\frac{10\lambda[8X'^2 - 2\pi X' - \pi^2]}{\sqrt{160 + 25\pi^2\lambda^2}} + 3[4X' - 3\pi] \right)$$

$$\mathcal{C}_{X'} := 10(5\pi^2\lambda^2 + \pi\lambda\sqrt{160 + 25\pi^2\lambda^2} + 8) + \frac{\sqrt{5\pi}(15\pi\lambda + \sqrt{160 + 25\pi^2\lambda^2})(5\pi\lambda^2[X' - \pi/4] - 4)}{\sqrt{5\pi\lambda^2[X' - \pi/4]^2 - 2[4X' - 3\pi]}}.$$

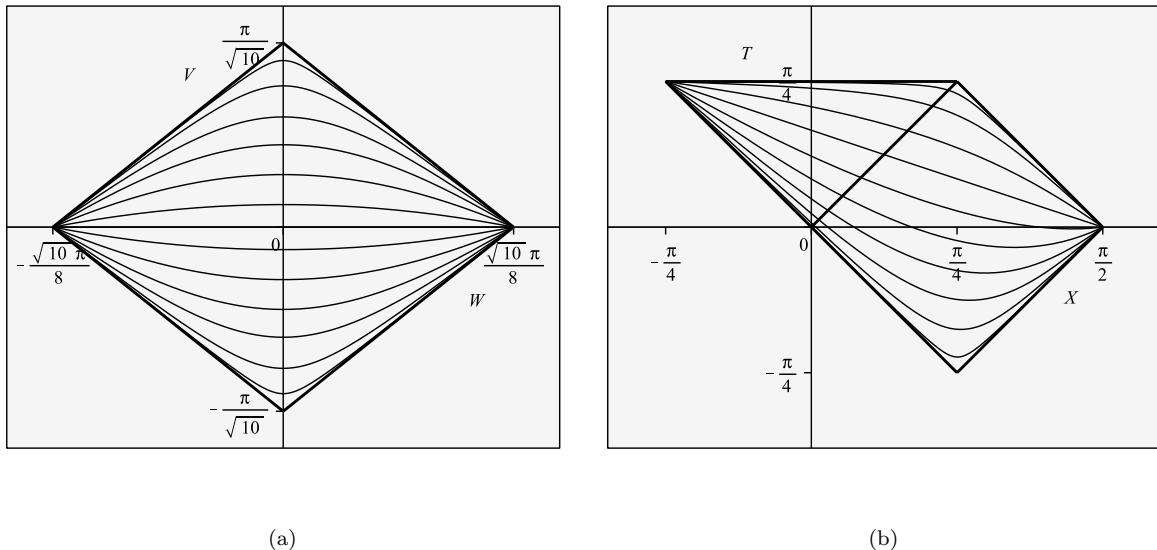


FIG. 3: Diamond representation of the extended Schwarzschild geometry with smooth functions $V_\lambda(W)$ defined by (16) for index values $\lambda \in \pm\{0, 0.2, 0.5, 0.9, 1.5, 3, 8\}$ (a) and Carter–Penrose diagram of the extended Schwarzschild geometry with level sets of the Cauchy temporal function specified in (17) for values $\lambda \in \{-10, -3.2, -1.6, -0.9, -0.45, -0.1, 0.28, 0.8, 2.1, 6.5\}$ (b).

As the $g_{\lambda\lambda}$ component of this metric is positive, it follows that the vector field ∂_λ is timelike in $B_I \cup B_{II}$. Besides, a direct computation shows that the time coordinate λ defined in (17) fulfills condition (15). Accordingly, the lapse conditions (C4) are satisfied. Moreover, since the metric component $g_{X'X'}$ is strictly negative, the induced metric on the level sets of λ is Riemannian as desired. In the Carter–Penrose diagram in FIG. 3(b), we illustrate the foliation of the analytic extension of the Schwarzschild geometry across the event horizon by the family of smooth, asymptotically flat, spacelike Cauchy hypersurfaces given by these level sets.

V. THE MINKOWSKI LIMIT

We discuss the possibility of taking the Minkowski limit of the family of horizon-penetrating characteristic coordinate systems for the extended Schwarzschild geometry introduced in Section III. In this limit, where the mass parameter $M \rightarrow 0$, both the transformation from the Boyer–Lindquist coordinates into the Eddington–Finkelstein double-null coordinates (2) as well as the transformation from the latter into the Kruskal–Szekeres double-null coordinates (4) become degenerate. More precisely, in the Minkowski limit, the Boyer–Lindquist blocks B_I and B_{II} turn into $\lim_{M \rightarrow 0} B_I = \mathbb{R} \times \mathbb{R}_{>0} \times S^2$ and $\lim_{M \rightarrow 0} B_{II} = \mathbb{R} \times \emptyset \times S^2$, with the future trapped region now being degenerate. Consequently, the Minkowski limit of the image of the Regge–Wheeler coordinate r_\star defined in (3) yields

$$\lim_{M \rightarrow 0} \begin{cases} \text{Ran}(r_\star) = \mathbb{R}_{>0} & \text{in } B_I \\ \text{Ran}(r_\star) = \emptyset & \text{in } B_{II}. \end{cases} \quad (18)$$

We remark that this coordinate is in general double-valued in the analytic extension $B_I \cup B_{II}$, and therefore invertible in B_I and B_{II} only separately. In the Minkowski limit, however, the Regge–Wheeler coordinate is, according to (18), not invertible in the Boyer–Lindquist block B_{II} . Hence, in this limit, the mapping (2) ceases to be bijective in B_{II} , and for this reason it is no longer a proper coordinate

transformation. With regard to the mapping (4), we find an even stronger form of degeneracy in the Minkowski limit that arises in both Boyer–Lindquist blocks, namely a reduction of the images of the Kruskal–Szekeres null coordinates U and V to point sets in B_I in addition to the above degeneracy in B_{II}

$$\lim_{M \rightarrow 0} \begin{cases} \text{Ran}(U) = \left\{ -\frac{\pi}{2}, -\frac{\pi}{4}, 0 \right\} & \text{and} & \text{Ran}(V) = \left\{ 0, \frac{\pi}{4}, \frac{\pi}{2} \right\} & \text{in } B_I \\ \text{Ran}(U) = \emptyset & & \text{and} & \text{Ran}(V) = \emptyset & \text{in } B_{II}. \end{cases}$$

Thus, in the Minkowski limit, the mapping (4) is not a bijection, and hence it fails to be a proper coordinate transformation as well. As a consequence, the Minkowski limit of the family of horizon-penetrating characteristic coordinate systems for the extended Schwarzschild geometry, which are based on these coordinate transformations, cannot be performed.

VI. GENERALIZATION TO THE NONEXTREME REISSNER–NORDSTRÖM GEOMETRY

We generalize our results to the analytic extension of the nonextreme Reissner–Nordström geometry up to the Cauchy horizon. This geometry is, like the analytic extension of the Schwarzschild geometry across the event horizon, a smooth, asymptotically flat and globally hyperbolic Lorentzian 4-manifold $(\mathfrak{M}, \mathbf{g})$, with \mathfrak{M} being homeomorphic to $\mathbb{R}^2 \times S^2$. It is, however, based on the unique 2-parameter family of exact, static, Petrov type D solutions \mathbf{g} of the more general Einstein–Maxwell equations, which can be used to analyze the final equilibrium state of the dynamical evolution of the exterior gravitational field of an electrically charged, spherically symmetric black hole. To this end, we perform the replacement of functions

$$1 - \frac{2M}{r} \rightarrow 1 - \frac{2M}{r} + \frac{Q^2}{r^2} =: \frac{\Delta(r)}{r^2}$$

in the Schwarzschild metric (1), where the parameter $Q \in \mathbb{R}$ denotes the electrical charge of the black hole geometry satisfying the relation $0 < |Q| < M$ and the two real-valued roots $r_{\pm} := M \pm \sqrt{M^2 - Q^2}$ of the function $\Delta: \mathbb{R}_{>0} \rightarrow \mathbb{R}_{\geq M}$ define an outer and an inner event horizon, respectively. This replacement gives rise to the Boyer–Lindquist representation of the nonextreme Reissner–Nordström metric [25, 29]

$$\mathbf{g} = \frac{\Delta}{r^2} dt \otimes dt - \frac{r^2}{\Delta} dr \otimes dr - r^2 \mathbf{g}_{S^2}. \quad (19)$$

The canonical analytic extension of the Reissner–Nordström geometry comprises the three connected Boyer–Lindquist blocks $B_I := \mathbb{R} \times \mathbb{R}_{>r_+} \times S^2$, $B_{II} := \mathbb{R} \times (r_-, r_+) \times S^2$, and $B_{III} := \mathbb{R} \times (0, r_-) \times S^2$. This structure is qualitatively different from the one of the Schwarzschild case, as the third Boyer–Lindquist block B_{III} contains a curvature singularity at $r = 0$ with timelike character and, more importantly for the present purpose, the inner event horizon at $r = r_-$ is a Cauchy horizon. Consequently, since our method for the construction of a family of horizon-penetrating characteristic coordinate systems requires the underlying Lorentzian manifold to be globally hyperbolic, we consider only the analytic extension $B_I \cup B_{II}$ of the nonextreme Reissner–Nordström geometry across the outer event horizon, up to the Cauchy horizon. Then, we transform the Boyer–Lindquist coordinates into compactified Kruskal–Szekeres-type coordinates

$$\mathfrak{T}^{\text{KST}} : \begin{cases} \mathbb{R} \times \mathbb{R}_{>0} \times (0, \pi) \times [0, 2\pi) \rightarrow \left(-\frac{\pi}{4}, \frac{\pi}{2} \right) \times \left(-\frac{\pi}{4}, \frac{\pi}{2} \right) \times (0, \pi) \times [0, 2\pi) \\ (t, r, \theta, \varphi) \mapsto (T, X, \theta, \varphi) \end{cases}$$

with

$$\begin{cases} T = \frac{1}{2} \arctan \left(\frac{\sinh(\alpha t)}{\cosh(\alpha r_*)} \right) & \text{and } X = -\frac{1}{2} \arctan \left(\frac{\cosh(\alpha t)}{\sinh(\alpha r_*)} \right) + \frac{\pi H(r_*)}{2} & \text{for } B_I \\ T = -\frac{1}{2} \arctan \left(\frac{\cosh(\alpha t)}{\sinh(\alpha r_*)} \right) + \frac{\pi H(r_*)}{2} & \text{and } X = -\frac{1}{2} \arctan \left(\frac{\sinh(\alpha t)}{\cosh(\alpha r_*)} \right) & \text{for } B_{II}, \end{cases}$$

where $T \in (|X - \pi/4| - \pi/4, -|X - \pi/4| + \pi/4)$ and $X \in (0, \pi/2)$ in B_I and $T \in (|X|, \pi/2 - |X|)$ and $X \in (-\pi/4, \pi/4)$ in B_{II} . Here, the Regge–Wheeler coordinate is defined as

$$r_* := r + \frac{r_+^2}{r_+ - r_-} \ln \left| \frac{r}{r_+} - 1 \right| - \frac{r_-^2}{r_+ - r_-} \ln \left(\frac{r}{r_-} - 1 \right),$$

$\alpha := (r_+ - r_-)/(2r_+^2)$ is a positive constant, and $H(r_*) := [1 + \text{sgn}(r_*)]/2$ is the Heaviside step function. The Reissner–Nordström metric (19) written in terms of these Kruskal–Szekeres-type coordinates takes the form

$$\mathbf{g} = \frac{r_+ r_- \left(\frac{r}{r_-} - 1\right)^{1-r_-^2/r_+^2} e^{-2\alpha r}}{\alpha^2 \cos^2(U) \cos^2(V) r^2} (dT \otimes dT - dX \otimes dX) - r^2 \mathbf{g}_{S^2}.$$

Next, we employ the method presented in Section III and work out the details of the specific sigmoid function application (16) introduced in Section IV within the present framework. However, as the Carter–Penrose diagram of the analytic extension $B_I \cup B_{II}$ of the nonextreme Reissner–Nordström geometry is already rectangularly shaped (see FIG. 4(a)), we may now omit transformation (9). Accordingly, carrying out all the necessary steps, we obtain the transformation from the above compactified Kruskal–Szekeres-type coordinates into the horizon-penetrating characteristic coordinates given by

$$\mathfrak{I}^{\text{CCRN}} : \begin{cases} \left(-\frac{\pi}{4}, \frac{\pi}{2}\right) \times \left(-\frac{\pi}{4}, \frac{\pi}{2}\right) \times (0, \pi) \times [0, 2\pi] \rightarrow \mathbb{R} \times \left(-\frac{\pi}{4}, \frac{\pi}{2}\right) \times (0, \pi) \times [0, 2\pi] \\ (T, X, \theta, \varphi) \mapsto (\lambda, X', \theta, \varphi) \end{cases}$$

with

$$\lambda = \frac{6T + 2X - \pi}{\sqrt{10 \left[(T - X)^2 - \frac{\pi^2}{4} \right] \left[T + X - \frac{\pi}{2} \right] [T + X]}} \quad \text{and} \quad X' = X. \quad (20)$$

Represented by means of these characteristic coordinates, the Reissner–Nordström metric reads

$$\begin{aligned} \mathbf{g} = & \frac{r_+ r_- \left(\frac{r}{r_-} - 1\right)^{1-r_-^2/r_+^2} e^{-2\alpha r}}{\alpha^2 \cos^2(U) \cos^2(V) r^2} \left[\frac{\mathcal{G}^2}{\lambda^2} d\lambda \otimes d\lambda + \frac{\mathcal{E} \mathcal{G}}{\sqrt{1 + \lambda^2 \mathcal{E}^2}} (d\lambda \otimes dX' + dX' \otimes d\lambda) - \frac{dX' \otimes dX'}{1 + \lambda^2 \mathcal{E}^2} \right] \\ & - r^2 \mathbf{g}_{S^2}, \end{aligned} \quad (21)$$

where

$$\mathcal{E} := \sqrt{\frac{5}{4}} \left[X' - \frac{\pi}{8} + \frac{1}{\lambda} \sqrt{\frac{1}{10} + \frac{\pi^2 \lambda^2}{64}} \right]$$

and

$$\mathcal{G} := \frac{1}{10\lambda} \left[\left(\frac{1}{10} + \frac{\pi^2 \lambda^2}{64} \right) (1 + \lambda^2 \mathcal{E}^2) \right]^{-1/2} \left[3\sqrt{1 + \lambda^2 \mathcal{E}^2} - \lambda \mathcal{E} - \sqrt{8 + \frac{5\pi^2 \lambda^2}{4}} \right].$$

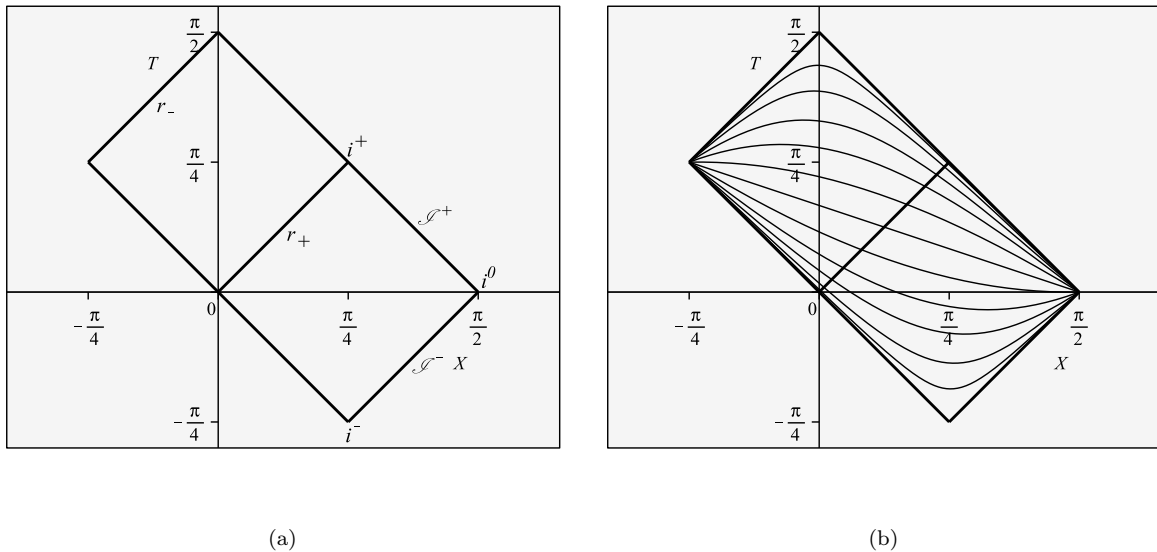


FIG. 4: Carter–Penrose diagram of the analytic extension of the nonextreme Reissner–Nordström geometry across the event horizon, up to the Cauchy horizon, (a) and the same Carter–Penrose diagram with level sets of the Cauchy temporal function defined in (20) for values $\lambda \in \pm\{0, 0.3, 0.65, 1.1, 2, 4\}$ (b).

From the positivity of the $g_{\lambda\lambda}$ component, we can deduce that the vector field ∂_λ is timelike in $B_I \cup B_{II}$. Also, computing the derivatives of the time coordinate λ defined in (20) with respect to the Kruskal–Szekeres-type variables T and X , we find that it fulfills condition (15). Hence, the lapse conditions (C4) are again satisfied. Furthermore, as the $g_{X'X'}$ component of (21) is strictly negative, one may easily establish that the induced metric on the level sets of λ is Riemannian. These level sets can be shown to have the Cauchy property by using a proof similar to the one of the Schwarzschild case (cf. Section III). As a consequence of all this, the time coordinate in (20) is a Cauchy temporal function. The foliation of the extended nonextreme Reissner–Nordström geometry $B_I \cup B_{II}$ by the family of smooth, asymptotically flat, spacelike Cauchy hypersurfaces given by the level sets of this temporal function is illustrated in the Carter–Penrose diagram in FIG. 4(b). We note in passing that the Schwarzschild limit $|Q| \rightarrow 0$ of the family of horizon-penetrating characteristic coordinate systems for the extended nonextreme Reissner–Nordström geometry is free from the type of degeneracies arising in the evaluation of the Minkowski limit $M \rightarrow 0$ of the Schwarzschild case discussed in Section V. Therefore, taking the Schwarzschild limit of the metric (21) yields

$$\lim_{|Q| \rightarrow 0} \mathbf{g} = \frac{32M^3 e^{-r/(2M)}}{\cos^2(U) \cos^2(V) r} \left[\frac{\mathcal{G}^2}{\lambda^2} d\lambda \otimes d\lambda + \frac{\mathcal{E} \mathcal{G}}{\sqrt{1 + \lambda^2 \mathcal{E}^2}} (d\lambda \otimes dX' + dX' \otimes d\lambda) - \frac{dX' \otimes dX'}{1 + \lambda^2 \mathcal{E}^2} \right] - r^2 \mathbf{g}_{S^2},$$

where the variables T and X in the definition (20) of the characteristic coordinates λ and X' are now given by (2)-(5) with the corresponding images. In this limit, however, since the time coordinate λ is a Cauchy temporal function adapted specifically to the rectangular shape of the Carter–Penrose diagram of the extended nonextreme Reissner–Nordström geometry, we find that its level sets do not correspond to spacelike Cauchy hypersurfaces in the Schwarzschild trapezoid. This stems from the fact that all level sets located in the region above the line $3T = -X + \pi/2$ eventually intersect the curvature singularity at $r = 0$. Hence, in the Schwarzschild limit, the original Cauchy property of the level sets of λ is lost, and we obtain only a foliation of the limiting spacetime by spacelike hypersurfaces.

VII. SUMMARY AND OUTLOOK

In this work, we derived a new family of horizon-penetrating characteristic coordinate systems for the Schwarzschild geometry featuring time coordinates that are Cauchy temporal functions. The level sets of these temporal functions give rise to foliations of the analytic extension of the Schwarzschild geometry across the event horizon by smooth, asymptotically flat, spacelike Cauchy hypersurfaces. More precisely, we introduced a geometric method of construction that employs certain structures inherent in the Carter–Penrose diagram of the extended Schwarzschild geometry, and worked out the details of a specific example based on sigmoid functions. We furthermore discussed the possibility of performing the Minkowski limit of this family of horizon-penetrating characteristic coordinate systems. Finally, we generalized our results to the case of the analytic extension of the nonextreme Reissner–Nordström geometry up to the Cauchy horizon and evaluated the corresponding Schwarzschild limit. We found that in this limit, the Cauchy property of the level sets of the new time coordinates gets lost. As smooth, spacelike Cauchy hypersurfaces embedded in – and foliating – a given spacetime are the natural subsets where initial data for the Einstein field equations is prescribed, coordinate systems of the above type are suitable for the study of the initial value formulations of the extended Schwarzschild and nonextreme Reissner–Nordström geometries, tracing their evolutions over time. Moreover, these coordinate systems may also be used to analyze causal and conformally invariant elements associated to these geometries in terms of data on a Cauchy surface.

In a future research paper, we plan on generalizing our method and results to the analytic extension of the stationary, axially symmetric nonextreme Kerr geometry up to the Cauchy horizon, which involves two significant challenges. On the one hand, due to the existence of nonvanishing cross terms, the Kerr metric does not have the particular product structure (7), making it impossible to locally relate the causal structure of the full Kerr geometry to that of the corresponding 2-dimensional Carter–Penrose diagram similar to the cases of the analytic extensions of the spherically symmetric black hole geometries. On the other hand, the time variable of the usual Kruskal–Szekeres-type coordinate system for the nonextreme Kerr geometry [7, 31] is not a temporal function, which is in contrast to the Kruskal–Szekeres time coordinates of the Schwarzschild and nonextreme Reissner–Nordström geometries. Since this aspect is, however, paramount for the present method, we are required to first modify the construction of the analytic Kruskal–Szekeres-type extension of the nonextreme Kerr geometry accordingly. Otherwise, we could also work with a different, more suitable horizon-penetrating coordinate system for the extended nonextreme Kerr geometry, which already contains a temporal function (for an example see the coordinate system analyzed in, e.g., [30]), as the basis for our geometric approach altogether. The use of such a coordinate system may, of course, lead to new obstacles that would have to be resolved eventually. In addition to this research project, we intend to apply our method to geometries other than black hole geometries as well, thereby focusing on conceptual issues and the applicability of the method itself and on the analyses of the associated characteristic coordinate systems.

Acknowledgments

The author is grateful to Miguel Sánchez for useful discussions and comments. This work was partially supported by the research project MTM2016-78807-C2-1-P funded by MINECO and ERDF.

[1] L. Andersson and M. S. Iriondo, “Existence of constant mean curvature hypersurfaces in asymptotically flat spacetimes,” *Annals of Global Analysis and Geometry* **17**, 503 (1999).

- [2] A. N. Bernal and M. Sánchez, “On smooth Cauchy hypersurfaces and Geroch’s splitting theorem,” *Communications in Mathematical Physics* **243**, 461 (2003).
- [3] A. N. Bernal and M. Sánchez, “Smoothness of time functions and the metric splitting of globally hyperbolic spacetimes,” *Communications in Mathematical Physics* **257**, 43 (2005).
- [4] R. H. Boyer and R. W. Lindquist, “Maximal analytic extension of the Kerr metric,” *Journal of Mathematical Physics* **8**, 265 (1967).
- [5] B. Carter, “The complete analytic extension of the Reissner–Nordström metric in the special case $e^2 = m^2$,” *Physics Letters* **21**, 423 (1966).
- [6] B. Carter, “Complete analytic extension of the symmetry axis of Kerr’s solution of Einstein’s equations,” *Physical Review* **141**, 1242 (1966).
- [7] S. Chandrasekhar, “The mathematical theory of black holes,” Oxford University Press (1983).
- [8] Y. Choquet–Bruhat, “General relativity and Einstein’s equations,” Oxford University Press (2009).
- [9] Y. Choquet–Bruhat and R. Geroch, “Global aspects of the Cauchy problem in general relativity,” *Communications in Mathematical Physics* **14**, 329 (1969).
- [10] P. T. Chruściel, “Elements of general relativity,” Birkhäuser (2020).
- [11] P. T. Chruściel, C. R. Özl, and S. J. Szybka, “Space-time diagrammatics,” *Physical Review D* **86**, 124041 (2012).
- [12] M. Dafermos and I. Rodnianski, “Lectures on black holes and linear waves,” *Clay Mathematics Proceedings* **17**, 97 (2013).
- [13] A. S. Eddington, “A comparison of Whitehead’s and Einstein’s formulae,” *Nature* **113**, 192 (1924).
- [14] D. Finkelstein, “Past–future asymmetry of the gravitational field of a point particle,” *Physical Review* **110**, 965 (1958).
- [15] R. Geroch, “Spinor structure of space-times in general relativity. I,” *Journal of Mathematical Physics* **9**, 1739 (1968).
- [16] R. Geroch, “Domain of dependence,” *Journal of Mathematical Physics* **11**, 437 (1970).
- [17] J. C. Graves and D. R. Brill, “Oscillatory character of Reissner–Nordström metric for an ideal charged wormhole,” *Physical Review* **120**, 1507 (1960).
- [18] J. B. Griffiths and J. Podolský, “Exact space-times in Einstein’s general relativity,” Cambridge University Press (2012).
- [19] A. Gullstrand, “Allgemeine Lösung des statischen Einkörperproblems in der Einsteinschen Gravitations-theorie,” *Arkiv för Matematik, Astronomi och Fysik* **16**, 1 (1922).
- [20] J. Haláček and T. Ledvinka, “The analytic conformal compactification of the Schwarzschild spacetime,” *Classical and Quantum Gravity* **31**, id. 015007 (2014).
- [21] M. D. Kruskal, “Maximal extension of Schwarzschild metric,” *Physical Review* **119**, 1743 (1960).
- [22] G. Lemaître, “L’Univers en expansion,” *Annales de la Société Scientifique de Bruxelles* **A53**, 51 (1933).
- [23] E. Minguzzi, “Lorentzian causality theory,” *Living Reviews in Relativity* **22**, 3 (2019).
- [24] E. Minguzzi and M. Sánchez, “The causal hierarchy of spacetimes,” *Recent developments in pseudo-Riemannian geometry*, ESI Lectures in Mathematics and Physics, 299 (2008).
- [25] G. Nordström, “On the energy of the gravitational field in Einstein’s theory,” *Koninklijke Nederlandsche Akademie van Wetenschappen Proceedings* **20**, 1238 (1918).
- [26] B. O’Neill, “The geometry of Kerr black holes,” Dover Publications (2014).
- [27] B. O’Neill, “Semi-Riemannian geometry with applications to relativity,” Academic Press (1983).
- [28] P. Painlevé, “La mécanique classique et la théorie de la relativité,” *Comptes Rendus de l’Académie des Sciences* **173**, 677 (1921).
- [29] H. Reissner, “Über die Eigengravitation des elektrischen Feldes nach der Einsteinschen Theorie,” *Annalen der Physik* **355**, 106 (1916).
- [30] C. Röken, “The massive Dirac equation in the Kerr geometry: Separability in Eddington–Finkelstein-type coordinates and asymptotics,” *General Relativity and Gravitation* **49**, 39 (2017).
- [31] C. Röken, “Kerr isolated horizons in Ashtekar and Ashtekar–Barbero connection variables,” *General Relativity and Gravitation* **49**, id. 114 (2017).
- [32] J. C. Schindler and A. Aguirre, “Algorithms for the explicit computation of Penrose diagrams,” *Classical and Quantum Gravity* **35**, id. 105019 (2018).
- [33] K. Schwarzschild, “Über das Gravitationsfeld eines Massenpunktes nach der Einsteinschen Theorie,” *Sitzungsberichte der Königlich Preussischen Akademie der Wissenschaften* **7**, 189 (1916).

- [34] H. Stephani, D. Kramer, M. MacCallum, C. Hoenselaers, and E. Herlt, “Exact solutions of Einstein’s field equations,” Cambridge University Press (2009).
- [35] G. Szekeres, “On the singularities of a Riemannian manifold,” *Publicationes Mathematicae Debrecen* **7**, 285 (1960).
- [36] R. M. Wald, “General relativity,” University of Chicago Press (1984).
- [37] R. M. Wald and V. Iyer, “Trapped surfaces in the Schwarzschild geometry and cosmic censorship,” *Physical Review D* **44**, R3719 (1991).
- [38] M. Walker, “Block diagrams and the extension of timelike two-surfaces,” *Journal of Mathematical Physics* **11**, 2280 (1970).